

# Delay-aided stochastic multiresonances on scale-free FitzHugh–Nagumo neuronal networks\*

Gan Chun-Biao(甘春标)<sup>a)</sup>, Perc Matjaž<sup>b)</sup>, and Wang Qing-Yun(王青云)<sup>c)d)†</sup>

<sup>a)</sup>*Institute of Applied Mechanics, School of Aeronautics and Astronautics, Zhejiang University, Hangzhou 310027, China*

<sup>b)</sup>*Department of Physics, Faculty of Natural Sciences and Mathematics, University of Maribor, Koroška Cesta 160, SI-2000 Maribor, Slovenia*

<sup>c)</sup>*School of Aeronautic and Engineering Science, Beijing University of Aeronautics and Astronautics, Beijing 100191, China*

<sup>d)</sup>*School of Statistics and Mathematics, Inner Mongolia Finance and Economics College, Huhhot 010071, China*

(Received 11 June 2009; revised manuscript received 16 October 2009)

The stochastic resonance in paced time-delayed scale-free FitzHugh–Nagumo (FHN) neuronal networks is investigated. We show that an intermediate intensity of additive noise is able to optimally assist the pacemaker in imposing its rhythm on the whole ensemble. Furthermore, we reveal that appropriately tuned delays can induce stochastic multiresonances, appearing at every integer multiple of the pacemaker's oscillation period. We conclude that fine-tuned delay lengths and locally acting pacemakers are vital for ensuring optimal conditions for stochastic resonance on complex neuronal networks.

**Keywords:** neuronal networks, delay, stochastic resonance

**PACC:** 0545

## 1. Introduction

The FitzHugh–Nagumo (FHN) equations are a simplified version of the Hodgkin–Huxley model of neuronal dynamics, capturing succinctly the activation and deactivation dynamics of a spiking neuron.<sup>[1]</sup> Due to its numerical efficiency, the FHN model has been used frequently for investigating the effects of noise on excitable neuronal-like dynamical systems. For example, the phenomenon of stochastic resonance and its enhancement due to coloured noise have been reported in Refs. [2] and [3]. Coherence resonance, where the spikes of the FHN neuron have maximal regularity in the presence of noise even without an external periodic signal, was presented in Refs. [4]–[6]. Moreover, coupled FHN neurons have been studied in Ref. [7], where it was shown that chemical synaptic coupling is more efficient than the well-known gap junctional coupling for local signal input detection. Slightly more exotic phenomena, like the doubly diversity-induced resonance,<sup>[8]</sup> array-enhanced coherence resonance,<sup>[9,10]</sup> and vibrational resonance<sup>[11,12]</sup> have also been studied in detail.

Since a single neuron in the vertebrate cortex can have links to as many as 10000 postsynaptic neu-

rons, and since neurons are known to be noisy analog units, understanding the effects of noise on networked excitable systems is of vital importance.<sup>[13,14]</sup> Related to this, the phenomena of stochastic and coherence resonance on complex neuronal networks became a vibrant topic as well. The stochastic resonance on excitable small-world networks was studied by means of the discrete Rulkov map<sup>[15]</sup> and the Hodgkin–Huxley model of neuronal dynamics.<sup>[16]</sup> Coherence resonance on Watts–Strogatz small-world Hodgkin–Huxley neuronal networks was also investigated, and it was found that increasing the randomness of the network topology leads to an enhancement of temporal coherence.<sup>[17]</sup> Moreover, Kwon *et al.*<sup>[18]</sup> showed that the coherence resonance can be considerably improved just by a small fraction of long-range connections for an intermediate coupling strength in a Watts–Strogatz small world neuronal network with spatially correlated noise. More recently, a new coherent excitation phenomenon has been reported in a heterogeneous network of coupled FHN neurons, where it has been shown that dynamical network rewiring may induce coherence resonance,<sup>[19]</sup> whereas from the experimental viewpoint, it has been shown that the

\*Project supported by the National Natural Science Foundation of China (Grant Nos. 10672140, 10972001 and 10832006). Matjaž Perc individually acknowledges the Support from the Slovenian Research Agency (Grant Nos. Z1-9629 and Z1-2032-2547).

†Corresponding author. E-mail: nmqingyun@163.com

© 2010 Chinese Physical Society and IOP Publishing Ltd

<http://www.iop.org/journals/cpb> <http://cpb.iphy.ac.cn>

spike-field-coherence in monkey prefrontal cortex is modulated by behaviour patterns.<sup>[20]</sup>

Using functional magnetic resonance imaging (fMRI), power-law distributions were obtained by linking correlated fMRI voxels,<sup>[21]</sup> and the robustness against simulated lesions of anatomic cortical networks has also been found relying mostly on the scale-free structure.<sup>[22]</sup> Recently, the dynamics of an excitable Greenberg–Hastings cellular automaton model on scale-free networks was studied.<sup>[23,24]</sup> In addition, information transmission delays are inherent to the nervous system because of the finite speed at which action potentials propagate across neuron axons, as well as due to time lapses occurring by both dendritic and synaptic processing.<sup>[25]</sup> Notably, it has been suggested that time delays can facilitate neural synchronisation and lead to many interesting and even unexpected dynamical phenomena, as described in Refs. [26]–[28]. Notably, it has been shown that dynamical relaying can yield zero time lag neuronal synchrony, thus overruling potentially hampering effects of long conduction delays.<sup>[29]</sup>

In the present paper, we aim to extend the scope of stochastic resonance on complex neuronal networks, particularly by considering scale-free interaction networks,<sup>[30]</sup> pacemakers, and time-delayed coupling. We elaborate the pacemaker-driven stochastic resonance in scale-free neuronal networks when the delay length is varied. We show that stochastic resonance via locally acting pacemakers is possible in the FHN neuronal network. In fact, the effects of the delay on stochastic resonance have been reported.<sup>[31]</sup> But more importantly, we present non-trivial effects induced by finite delays, which may induce stochastic multiresonances provided that the delay length is adequately adjusted. This is primarily attributed to the emergence of locking between the delay length and the global resonant oscillation frequency<sup>[32]</sup> of individual FHN neurons constituting the scale-free network as well as the frequency of the pacemaker.

The remainder of this paper is organised as follows. In the next section we describe the FHN model<sup>[1]</sup> on the scale-free network,<sup>[30]</sup> as well as the time-delayed coupling scheme and the measure for stochastic resonance. Subsequently, the main results are presented and summarised.

## 2. Mathematical model and setup

In order to simulate the stochastic neuronal dynamics on the scale-free network effectively, we employ the FHN equations.<sup>[1]</sup> The spatiotemporal evolution of the neuronal network to be studied, along with additive Gaussian noise  $\xi_i(t)$  and delay  $\tau$ , is governed by the following equations

$$\begin{aligned} \rho \dot{x}_i &= x_i - x_i^3/3 - y_i + \sigma \xi_i(t) \\ &+ D \sum_j \varepsilon^{i,j} [x_j(t - \tau) - x_i(t)], \quad (1) \\ \dot{y}_i &= x_i + a, \quad (i = 1, \dots, L), \end{aligned}$$

where  $x$  and  $y$  represent the fast activation variable and the slow recovery variable, respectively;  $\rho$  (we fix  $\rho = 0.01$  unless stated otherwise) determines the inherent time scale of the local dynamics. Parameter  $a$  determines the behaviour of the system. In the absence of noise, for  $a > 1.0$  the FHN model is excitable, and for  $a < 1.0$  it shows oscillatory behaviour. At the bifurcation  $a = 1.0$ , the stability of the only fixed point is lost.<sup>[4]</sup> Presently, we set  $a = 1.005$  and initiate each neuron from steady state initial conditions, so that the additive spatiotemporal Gaussian noise  $\xi_i(t)$ , having mean  $\langle \xi_i(t) \rangle = 0$  and autocorrelation  $\langle \xi_i(t) \xi_j(t') \rangle = \delta_{ij} \delta(t - t')$ , acts as the only source of large-amplitude excitations.  $D$  is the coupling strength, the parameter  $\sigma$  determines the noise intensity, and  $\tau$  is the afore-mentioned delay length. The latter two parameters will be the focus of attention within this work.

It remains of interest to mathematically introduce the pacemaker, which takes the form of a periodic force defined by

$$\pi^{(r)} = A \cos(\omega t), \quad (2)$$

where the superscript  $r$  denotes a chosen excitable neuron among all the  $N = 200$  neurons constituting the excitable array, to which the pacemaker is introduced as an additive term to the variable  $y_i$ . Furthermore,  $A$  is the amplitude of the periodic sub-threshold pacemaker, presently set to  $A = 0.01$ , and  $\omega$  ( $\omega = 2\pi/T$ ;  $T$  being the oscillation period) is its angular frequency. The appropriate value of  $T$  depends on the global resonant oscillation frequency<sup>[32]</sup> of each individual FHN model; notably the two should be comparable for optimal results, which under the above-stated parameter values leads to  $T = 3.6$ . We will use this value of  $T$  unless stated otherwise.

As the interaction base between the FHN neurons we use the scale-free network generated via growth and preferential attachment as proposed by Barabási and Albert,<sup>[30]</sup> consisting of  $L = 200$  vertices. Each vertex corresponds to one neuron, whose dynamics is governed by the noise-driven FHN model. In Eq. (1)  $\varepsilon^{i,j} = 1$  if neuron  $i$  is coupled to neuron  $j$  and  $\varepsilon^{i,j} = 0$  otherwise. Following Ref. [30], the preferential attachment is introduced via the probability  $\Pi$ , which states that a new vertex will be connected to vertex  $i$  depending on its degree  $k_i$  according to  $\Pi(k_i) = k_i / \sum_j k_j$ . This growth and preferential attachment scheme yields a network with an average degree  $k_{av} = (1/L) \sum_i k_i$ , and a power-law degree distribution with the slope of the line equal to  $-2.9$  on a double-logarithmic graph. Notably, analytical estimations predict that the slope of the line equals  $-3$ . We will use networks having  $k_{av} = 4$  throughout this work.

To quantitatively characterise the collective response of the neuronal network, we introduce the average membrane potential  $X(t) = \frac{1}{L} \sum_{i=1}^L x_i(t)$  as the main output to be examined further. The correlation of the average membrane potential  $X(t)$  with frequency of the pacemaker  $\omega = 2\pi/T$  is computed via the Fourier coefficients

$$Q_{\sin} = \frac{2}{NT} \int_0^{NT} X(t) \sin(\omega t) dt, \quad (3)$$

$$Q_{\cos} = \frac{2}{NT} \int_0^{NT} X(t) \cos(\omega t) dt, \quad (4)$$

where  $N = 200$  is the number of periods of the pacemaker used for calculation presented below. In this paper, we use  $Q = \sqrt{Q_{\sin}^2 + Q_{\cos}^2}$  as a numerically effective measure for stochastic resonance, capturing succinctly the collective spatiotemporal behaviour of the neuronal network considered and its correlation with the pacemaker rhythm. In general,  $Q$  can exhibit a bell-shaped profile as a key parameter (for example  $\sigma$ ) is varied, thereby indicating the occurrence of stochastic resonance. Importantly, since the generation of scale-free networks has inherent random ingredients, which can be additionally amplified by individual vertex (neuron) pacing, the final results shown below were averaged over 30 independent runs for each set of applicable parameter values to warrant appropriate accuracy.

### 3. Results

We start by setting  $\tau = 0$  and introducing the pacemaker to the neuron with the lowest degree  $k_{\min}$  within the network, thus  $r = i(k_{\min})$ . Space-time plots for different  $\sigma$  are presented in Fig. 1. It is shown that smaller  $\sigma$  fails to evoke continuous excitations [see Fig. 1(a)]. As  $\sigma$  increases, regular spatiotemporal patterns can appear [see Figs. 1(b)–1(d)]. Further investigation shows that the excitatory fronts follow the pacemaker rhythm (oscillation period is  $T = 3.6$ ) only by an intermediate value of  $\sigma$  [see Fig. 1(c)]. From Fig. 1(b), the regular wave period is 3.73, which is greater than  $T = 3.6$ ; while in Fig. 1(d) the regular wave period is 3.55, and is smaller than  $T = 3.6$ . Larger noises exceeding the optimal value, however, have the ability of initiating excitations on their own (even when the pacemaker is not firing), thus again failing to conform to the weakly imposed rhythm or further still, completely overruling the deterministic dynamics [see Fig. 1(e)]. The presented results therefore indicate a classical stochastic resonance scenario, where an intermediate noise intensity warrants the best response of the system to a weak external deterministic forcing. Notably, qualitatively identical results are obtained if the pacemaker is introduced to the neuron with the largest degree  $r = i(k_{\max})$  within the scale-free network. It is next of interest to assess these observations quantitatively.

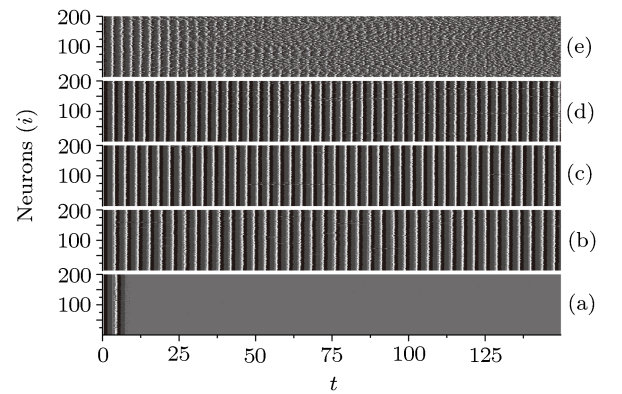


**Fig. 1.** Space-time plots obtained at  $\tau = 0$  and  $D = 0.01$  for different  $\sigma$ : (a) 0.008, (b) 0.05, (c) 0.15, (d) 0.5 and (e) 1. In all panels the colour profile is linear, black depicting  $x_i(t) = -2.0$  and white  $x_i(t) = 2.0$ , with eight shades of grey in between.

To establish the described pacemaker-driven stochastic resonance more precisely, we consider the dependence of  $Q$  on  $\sigma$  in Fig. 2(a) for different options with respect to the places of the pacemaker. It can be observed that, irrespective of whether the pacemaker is introduced to the neuron with the minimal

$r = i(k_{\min})$  or the maximal degree  $r = i(k_{\max})$ , there exists an intermediate optimal noise intensity  $\sigma$  for which  $Q$  is maximal, thus exhibiting a bell-shaped dependence characteristic for stochastic resonance.

Before turning to the impact of finite information transmission delays  $\tau$ , we investigate in Fig. 2(b) stochastic resonance in the transition to the strong coupling region (high values of  $D$ ). Results are presented for  $r = i(k_{\min})$  but are qualitatively identical also for  $r = i(k_{\max})$  (not shown). Evidently, the stochastic resonance phenomenon prevails irre-

spective of  $D$ , only that the optimal value of  $\sigma$  shifts to slightly higher values upon its increase. Thus, it can be concluded that the pacemaker driven stochastic resonance on scale-free neuronal networks is a robust phenomenon, occurring largely independently of the particular places of the pacemaker or the strength of the coupling. In what follows we will therefore focus on the individually paced noise-driven scale-free neuronal networks, wherein one of the neurons having the lowest degree will be chosen as the input for the deterministic forcing.

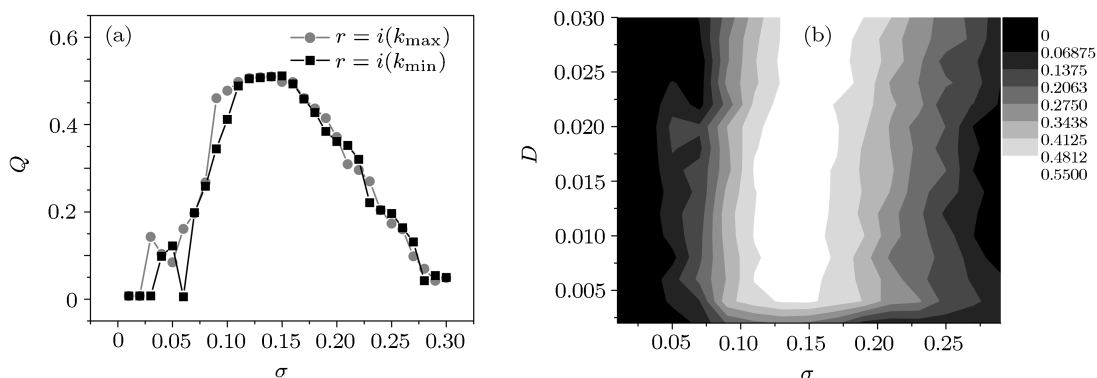


**Fig. 2.** (a) Dependence of  $Q$  on  $\sigma$  at  $\tau = 0$  and  $D = 0.01$  for different places of the pacemaker within the scale-free network (see also main text for further details). (b) Dependence of  $Q$  on  $\sigma$  and  $D$  at  $\tau = 0$  when the pacemaker is introduced to one of the neurons having the lowest degree [ $r = i(k_{\min})$ ].

Next, we present in Fig. 3 the space-time plots obtained for different  $\tau$  while keeping the coupling strength  $D = 0.01$  and the noise intensity  $\sigma = 0.15$  fixed. The results shown in the five panels of Fig. 3 illustrate the spatiotemporal dynamics of neurons on the studied scale-free neuronal network for  $r = i(k_{\min})$ . Upon careful visual inspection, an intermittent pattern of regularity and disorder can be inferred upon increasing  $\tau$ . In particular, while for  $\tau = 3.6$  [panel (b)] and  $\tau = 7.2$  [panel (d)] the excitatory fronts are synchronous and largely obeying the pacemaker rhythm, for  $\tau = 1.5$  [panel (a)],  $\tau = 5.0$  [panel (c)] and  $\tau = 8.0$  [panel (e)] the regularity is either completely lost or at least the excitatory fronts become ragged and lose synchrony with the imposed frequency. Indeed, the information-transmission-delay-induced transitions to ordered spatiotemporal dynamics on scale-free neuronal networks appear intermittently at roughly integer multiples of the period of the pacemaker,  $T = 3.6$  throughout this work unless stated otherwise. Importantly,  $T = 3.6$

corresponds rather accurately to the global resonant oscillation period<sup>[32]</sup> of the FHN neuron for the currently used parameter values  $\rho = 0.01$ . By setting

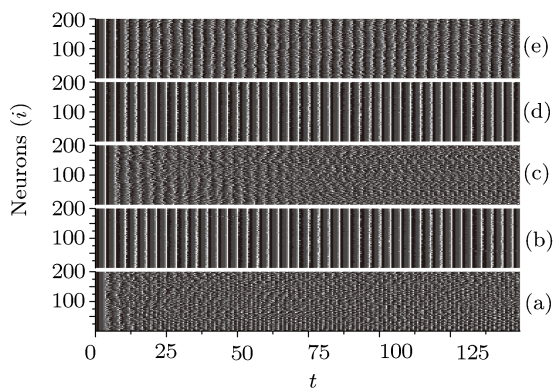


**Fig. 3.** Space-time plots obtained at  $D = 0.01$  and  $\sigma = 0.15$  for different  $\tau$ : (a) 1.5, (b) 3.6, (c) 5, (d) 7.2 and (e) 8.0. In all panels the colour profile is linear, black depicting  $x_i(t) = -2.0$  and white  $x_i(t) = 2.0$ , with eight shades of grey in between.

$T$  largely different from the global resonant oscillation period of individual neurons, however, the inter-

mittent outline presented in Fig. 3 can no longer be observed. Visual investigations of Fig. 3 thus reveal that regular and irregular front propagation appears intermittently as the delay is increased, hence indicating that finite information transmission delays might play a central role by the generation of spatiotemporal order of neuronal activity on scale-free networks in accordance with a weak localised deterministic input, provided that the latter is so adjusted as to approximately agree with the global resonant oscillation frequency of constitutive neurons.

To account for the above visual interpretations quantitatively, we adjust the local dynamics of each neuron (thus far we have not varied this) by varying  $\rho$ , in turn affecting the speed of the temporal evolution of  $x_i(t)$  and consequently also the global resonant frequency. At the same time, we adjust the oscillation period of the pacemaker  $T$  correspondingly. In particular, we consider two different cases, namely  $\rho = 0.02$  and  $\rho = 0.01$ , and change the oscillation period of the pacemaker to  $T = 4.2$  and  $T = 3.6$ , respectively. These  $T$  are in good agreement with the global resonant frequency of an individual neuron for the corresponding values of  $\rho$ . Notably, the global resonant frequency can be extracted from the FHN model by calculating the Fourier transform of noise-driven oscillations, as described in Ref. [32]. Results presented in Fig. 4 show that, in accordance with the visual inspection of Fig. 3, multiple resonances in  $Q$  with the increase of  $\tau$  are obtained by setting  $\sigma$  and  $D$ . Following the established terminology, these can be termed appropriately as delay-aided stochastic multiresonances on scale-free neuronal networks. Moreover, it is clear that the particular locations of the maxima of  $Q$  shift to different values of  $\tau$  as  $\rho$  and  $T$  are varied. Crucially however, it is always so when the locking between  $\tau$  and integer multiples of  $T$  is preserved. Thus, the resonances in dependence on  $\tau$  appear at integer multiples of  $T$  if only the latter is close to the global resonant oscillation period of the individual neurons. On the other hand, values of  $\tau$  outside the regions of multiple integers of  $T$  impair the stochastic resonance significantly, as can be inferred from the rather sharp descents of  $Q$  towards smaller values as soon as the optimal  $\tau$ 's are replaced by other values. We therefore conclude that the delay-induced stochastic resonances of neuronal activity are due to the locking between the length of the delay  $\tau$  and the predominant oscillation period of individual neurons constituting the scale-free network. This is valid independently of the

particular places of the pacemaker, and also for globally paced scale-free neuronal networks with different coupling strengths.

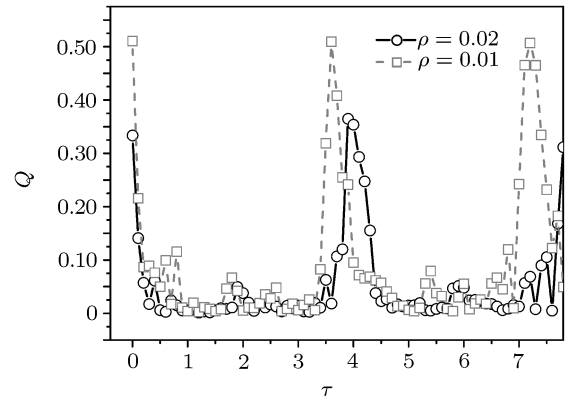


Fig. 4. Dependence of  $Q$  on  $\tau$  for different  $\rho$  (see also main text for further details) when the pacemaker is introduced to one of the neurons with the lowest degree [ $r = i(k_{\min})$ ]. Where applicable, other parameter values are the same as those in Fig. 3.

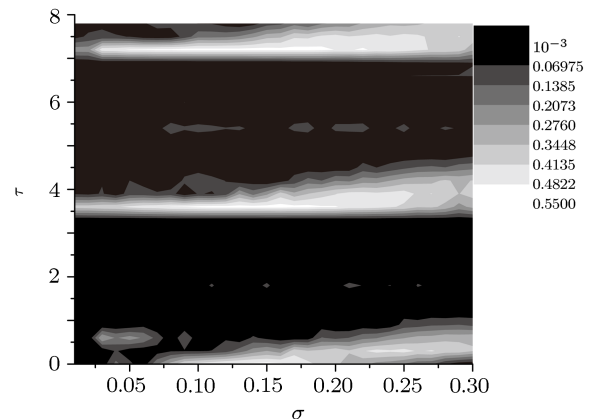


Fig. 5. Contour plots of  $Q$  versus  $\tau$  and  $\sigma$  when the pacemaker is introduced to one of the neurons with the lowest degree [ $r = i(k_{\min})$ ] and  $D = 0.01$ . Further parameter values are:  $\rho = 0.01$ ,  $T = 3.6$ .

Finally, we present results where the above-outlined dependences can be observed at a glance. Figure 5 shows the dependence of  $Q$  on  $\sigma$  and  $\tau$  for  $\rho = 0.01$ . Stochastic multiresonances are clearly eligible as narrow white-shaded regions, appearing roughly at integer multiples of  $\tau = 3.6$  across suitable spans of  $\sigma$ . It is worthwhile emphasising that the very narrow region of optimal  $\tau$ , especially if compared to the rather broad span of  $\sigma$  that still ensures reasonably high  $Q$ , suggests that fine-tuned delays might be central for the efficient recognition of weak localised external signals. Also notably, some faintly expressed regions of stochastic resonance can be observed for small  $\tau$  ( $\approx 0.4$ ). However, these are mostly the consequence of the fact that short delay lengths do not

influence the neuronal dynamics strongly enough to fully prohibit noise-induced correlations between the pacemaker and the neuronal dynamics; and in turn they occasionally yield results similar to the  $\tau = 0$  case, but only at substantially higher noise intensities which are needed to compensate for the disturbing impact of non-optimal information transmission delays. Moreover, for other forcing frequencies of the pacemaker we have performed similar investigation, yet only when the pacemaker frequency is very close to the global resonant frequency of individual neurons forming the scale-free network can stochastic multiresonances be observed at integer multiples of the forcing period.

## 4. Summary and discussion

In summary, we have studied stochastic resonance phenomena on paced scale-free FHN neuronal networks as the noise intensity and the delay length are

varied. We find that stochastic resonance occurs irrespective of the location of the pacemaker. Furthermore, as we introduce time-delayed coupling with finite  $\tau$ , we can observe stochastic multiresonances upon fine-tuning of the delay length, which appear at every multiple of the forcing frequency if the latter is close enough to the global resonant oscillation frequency of individual neurons. More precisely, the stochastic multiresonances appear in an intermittent fashion as the delay increases, whereby the intermittency is a direct consequence of the on/off locking between the forcing frequency and the information transmission delay length. Thus, we have shown that noise and information transmission delays can play complementary roles in warranting optimal detection of weak localised stimuli in neuronal scale-free networks via stochastic resonance. We hope that our study will be useful when striving towards further advances in understanding neuronal dynamics on complex networks.

## References

- [1] Zhang S H and Shen K 2002 *Chin. Phys.* **11** 894
- [2] Nagumo J, Arimoto S and Yoshizawa S 1962 *Proc IRE.* **50** 2061
- [3] Gong P L and Xu J X 2001 *Phys. Rev. E* **63** 031906
- [4] Nozaki D and Yamamoto Y 1998 *Phys. Lett. A* **243** 281
- [5] Pikovsky A S and Kurths J 1997 *Phys. Rev. E* **78** 775
- [6] Horikawa Y 2001 *Phys. Rev. E* **64** 031950
- [7] Escalona J, Santos G J E and Parmananda P 2007 *Phys. Rev. E* **76** 016213
- [8] Li X M, Wang J and Hu W H 2007 *Phys. Rev. E* **76** 041902
- [9] Gassel M, Glatt E and Kaiser F 2007 *Phys. Rev. E* **76** 016203
- [10] Zhou C S, Kurths J and Hu B 2003 *Phys. Rev. E* **67** 030101
- [11] Shinohara Y, Kanamaru T, Suzuki H, Horita T and Aihara K 2002 *Phys. Rev. E* **65** 051906
- [12] Cubero D, Baltan J P and Casado-Pascual J 2006 *Phys. Rev. E* **73** 061102
- [13] Deng B, Wang J and Wei X L 2009 *Chaos* **19** 013117
- [14] Kinouchi O and Copelli M 2006 *Nature Phys.* **2** 348
- [15] Ribeiro T L and Copelli M 2008 *Phys. Rev. E* **77** 051911
- [16] Perc M 2007 *Phys. Rev. E* **76** 066203
- [17] Ozer M, Perc M and Uzuntarla M 2009 *Phys. Lett. A* **373** 964
- [18] Kwon O and Moon H T 2002 *Phys. Lett. A* **298** 319
- [19] Kwon O, Jo H H and Moon H T 2005 *Phys. Rev. E* **72** 066121
- [20] Jiang M and Ma P 2009 *Chaos* **19** 013115
- [21] Wu W, Wheeler D W, Staedler E S, Munk M H J and Pipa G 2008 *Neuro Rep.* **19** 235
- [22] Eguíluz V M, Chialvo D R, Cecchi G A, Baliki M and Apkarian A V 2005 *Phys. Rev. Lett.* **94** 018102
- [23] Kaiser M, Martin R, Andras P and Young M P 2007 *Eur. J. Neurosci.* **25** 3185
- [24] Wu A C, Xu X J and Wang Y H 2007 *Phys. Rev. E* **75** 032901
- [25] Copelli M and Campos P R A 2007 *Eur. Phys. J. B* **56** 273
- [26] Kandel E R, Schwartz J H and Jessell T M 1991 *Principles of Neural Science* (Amsterdam: Elsevier)
- [27] Wang Q Y and Lu Q S 2005 *Chin. Phys. Lett.* **22** 543
- [28] Rossoni E, Chen Y H, Ding M Z and Feng J F 2005 *Phys. Rev. E* **71** 061904
- [29] Wang Q Y, Duan Z S, Perc M and Chen G R 2008 *Europhys. Lett.* **78** 50008
- [30] Vicente R, Golo L L, Mirasso C R, Fischer I and Pipa G 2008 *Proc. Nat. Acad. Sci. USA* **105** 17157
- [31] Barabási A L and Albert R 1999 *Science* **286** 509
- [32] Du L C and Mei D C 2009 *Chin. Phys. B* **18** 946
- [33] Perc M and Marhl M 2005 *Phys. Rev. E* **71** 026229